Acta Crystallographica Section C
Crystal Structure Communications
ISSN 0108-2701

1-[2-(2,6-Diisopropylanilino)-1-naphthyl]isoquinoline

Ruth H. Howard,‡ Nicola Theobald, Manfred Bochmann and Joseph A. Wright*

School of Chemistry, University of East Anglia, Norwich NR4 7TJ, England
Correspondence e-mail: joseph.wright@uea.ac.uk

Received 10 May 2010
Accepted 18 May 2010
Online 26 May 2010

The molecule of the title compound, $C_{31}H_{30}N_2$, contains a single intramolecular hydrogen bond, in contrast with the related *N*-methyl compound which exists as hydrogen-bonded dimers in the solid state [Cortright, Huffman, Yoder, Coalter & Johnston (2004). *Organometallics*, **23**, 2238–2250]. Application of the density functional theory programs *CASTEP* and *DMol*^{3} allows accurate assignment of the location of the H atoms in the structure.

Comment

The 1-isoquinolyl-2-aminonaphthalene (IAN) ligands were developed by Johnston and co-workers (Cortright & Johnston, 2002; Cortright, Yoder & Johnston, 2004). Ligands of this type are bidentate, having one amine and one imine-equivalent coordinating group, and they are axially chiral, as in the classic BINOL-derived family (BINOL is 1,1′-bi-2-naphthol), since rotation about the naphthyl–isoquinolyl linkage is restricted by the H atoms β to this bond. Formation of a metal complex from an IAN ligand leads to the formation of a six-membered chelate ring with the metal in the centre.

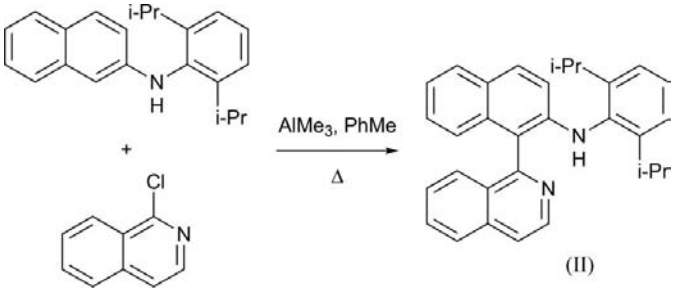

These IAN ligands have been applied to the coordination of zirconium and aluminium with the resulting complexes used in a variety of transformations, including olefin polymerization and addition of diethylzinc to benzaldehyde (Cortright, Huffman *et al.*, 2004; Cortright, Coalter *et al.*, 2004). However, most of this work was carried out with ligands in which the *R* group of the amine N atom (Fig. 1) was small, for example, methyl [ligand (I)]. Intrigued by the possibility that increasing the bulk of the *R* group could improve catalytic activity, we have investigated the use of the title compound, (II), containing the bulky 2,6-diisopropylphenyl group on the amine N atom. This molecule has been reported by Johnston and co-workers (Cortright, Huffman *et al.*, 2004) but not pursued in a catalytic context.

Synthesis of (II) followed the literature route, after which X-ray quality crystals could be obtained from a concentrated dichloromethane solution. The structure of (II) (Fig. 2) reveals that the molecule exists as a monomer in the solid state with a single intramolecular hydrogen bond (Table 1). This is in sharp contrast with the reported structure for (I) (Cortright, Huffman *et al.*, 2004), which exists a hydrogen-bonded dimer in the solid state. The dimer contains two nonsymmetry-related molecules, and exhibits one shorter and one longer hydrogen bond (N···H distances = 2.051 and 2.246 Å, respectively). The intramolecular N···H distance in (II) (2.51 Å) is significantly longer, suggesting a much less favourable interaction. Presumably, the additional steric requirement of the bulky aryl group prevents the formation of an intermolecular hydrogen bond.

Reaction of (II) with BuLi followed by MeMgCl in tetrahydrofuran yields a material which gives satisfactory spec-

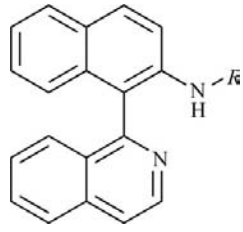

Figure 1
The general structure of the IAN ligand family. For (I), *R* = Me, and for (II), *R* = 2,6-^{i}Pr$_2$C$_6$H$_3$.

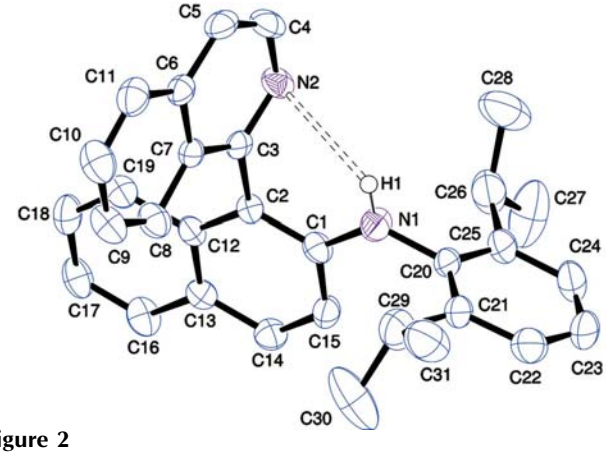

Figure 2
The structure of (II), showing the atom-numbering scheme. Displacement ellipsoids are drawn at the 50% probability level, and H atoms except H2 and the minor component of the disordered isopropyl group have been omitted for clarity. The dashed lines indicate the intramolecular hydrogen bond.

‡ Current address: Accelrys Ltd, 334 Cambridge Science Park, Cambridge CB4 0WN, England.

  doi:10.1107/S0108270110018433

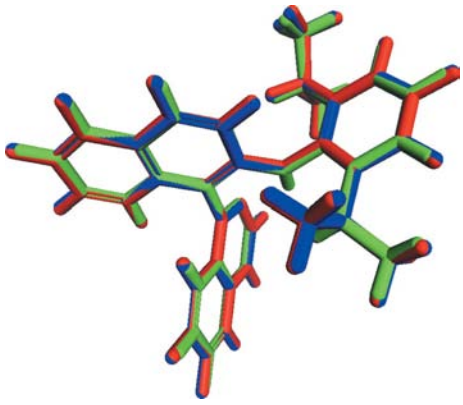

Figure 3
An overlay of the experimental structure of (II) (light shading; green in the electronic version of the paper) with that calculated using the *Dmol*^{3} (dark shading/blue) and *CASTEP* (mid-shading/red) methods.

troscopic data to confirm the loss of methane and the formation of a mono-ligand complex. At present, we have been unable to grow X-ray quality crystals of this material to confirm this assignment. However, a similar reaction with $AlEt_3$ does not lead to the loss of an alkyl group, although the spectroscopic data do suggest that an adduct is formed. It therefore seems that the additional bulk of the aryl group severely hinders deprotonation of the amine group in (II) compared with the more reactive (I).

H atoms have low scattering power, the electron density associated with the atom is not usually centred at the nucleus, and H atoms tend to have higher librational amplitudes than other nuclei (Sheldrick, 1997). As a result, the placement of H atoms in X-ray structures is usually carried out by applying a riding model based on established geometric parameters. The combination of structural data from X-ray diffraction with *ab initio* calculations can be used to provide reliable H-atom positions (Milman & Winkler, 2001). Compound (II) was an attractive target to investigate the application of this approach to the location of the H atoms, as it presents H atoms with a number of different bonding modes, including hydrogen bonding, in a well defined structure.

The density functional theory (DFT) programs *CASTEP* (Clark *et al.*, 2005) and *DMol*^{3} (Delley, 2000), as implemented in *Materials Studio* (Accelrys, 2009), were used to perform these calculations. The lattice parameters were not varied as the experimentally determined parameters are sufficiently accurate. A comparison of an all-electron (*DMol*^{3}) and a pseudopotential (*CASTEP*) approach provides additional confidence that the DFT results for this crystal structure do not depend on the implementation details of a particular DFT technique.

Initial comparison of the fractional coordinates of selected heavy atoms indicates the high accuracy of their experimentally determined positions (Table 2). Overlaying the experimentally determined structure (light shading/green) with the *DMol*^{3} (dark shading/blue) and *CASTEP* (mid-shading/red) optimized structures illustrates the accuracy of the heavy-atom positions and the displacement of the H atoms (Fig. 3). Analysis of the lengths of bonds to H atoms shows that, as expected, both theoretical methods calculate the positions of the H atoms at greater distances from the heavy atoms than the riding-model positions (Table 3). Looking at the average differences between the experimental and calculated values (Table 4), it is clear that both DFT methods give very similar results. For both DFT methods used, the aromatic C—H distances show the greatest variation from those used in the X-ray refinement, where H atoms where placed using established geometric parameters and refined using a riding model. The closest agreement between the DFT and X-ray model C—H distances was seen for methine C—H bonds.

By combining DFT methods with experimental locations for non-H atoms, a model for (II) which locates the H atoms accurately is available. This provides a useful alternative to more difficult to access methods for accurate H-atom location in solids for which X-ray quality single crystals are available.

Experimental

Compound (II) was prepared according to the literature method of Cortright, Huffman *et al.* (2004). Crystals of (II) suitable for X-ray diffraction studies were grown from a concentrated dichloromethane solution.

Crystal data

$C_{31}H_{30}N_2$
M_r = 430.57
Orthorhombic, $P2_12_12_1$
a = 9.0996 (10) Å
b = 11.2154 (12) Å
c = 23.974 (3) Å
V = 2446.7 (5) Å^3
Z = 4
Mo $K\alpha$ radiation
μ = 0.07 mm^{-1}
T = 140 K
0.30 × 0.10 × 0.10 mm

Data collection

Oxford Xcalibur3 CCD area-detector diffractometer
28412 measured reflections
2579 independent reflections
1584 reflections with $I > 2\sigma(I)$
R_{int} = 0.178

Refinement

$R[F^2 > 2\sigma(F^2)]$ = 0.056
$wR(F^2)$ = 0.101
S = 0.95
2579 reflections
311 parameters
3 restraints
H-atom parameters constrained
$\Delta\rho_{max}$ = 0.15 e Å^{-3}
$\Delta\rho_{min}$ = −0.17 e Å^{-3}

Table 1
Hydrogen-bond geometry (Å, °).

D—H···A	D—H	H···A	D···A	D—H···A
N1—H1···N2	0.88	2.51	3.070 (4)	122

Table 2
Fractional coordinates of selected heavy atoms.

Atom	Experimental (x, y, z)	*CASTEP* (x, y, z)	*DMol*^{3} (x, y, z)
N1	(0.3355, 0.3474, 0.8822)	(0.3445, 0.3495, 0.8821)	(0.3371, 0.3484, 0.8822)
N2	(0.2487, 0.0978, 0.8408)	(0.2509, 0.1019, 0.8435)	(0.2466, 0.0994, 0.8431)
C1	(0.3672, 0.3546, 0.8257)	(0.3717, 0.3579, 0.8255)	(0.3664, 0.3566, 0.8256)
C2	(0.3028, 0.2755, 0.7889)	(0.3061, 0.2768, 0.7884)	(0.3026, 0.2746, 0.7884)
C3	(0.1955, 0.1863, 0.8097)	(0.1989, 0.1888, 0.8105)	0.1950, 0.1862, 0.8103)
C20	(0.3942, 0.4267, 0.9234)	(0.4006, 0.4294, 0.9235)	(0.3956, 0.4279, 0.9234)

Table 3
C—H and N—H bond lengths (Å) in (II) from X-ray experiment and DFT calculations.

Bond	*CASTEP*	*DMol*^{3}
Aryl C—H (riding model 0.95 Å)		
C4—H4	1.093	1.092
C5—H5	1.091	1.091
C8—H8	1.090	1.090
C9—H9	1.090	1.089
C10—H10	1.090	1.089
C11—H11	1.089	1.089
C14—H14	1.091	1.091
C15—H15	1.090	1.090
C16—H16	1.093	1.092
C17—H17	1.089	1.088
C18—H18	1.091	1.091
C19—H19	1.091	1.091
C22—H22	1.091	1.090
C23—H23	1.090	1.090
C24—H24	1.090	1.090
Methine C—H (riding model 1.00 Å)		
C26—H26	1.102	1.100
C29—H29	1.100	1.099
Methyl C—H (riding model 0.98 Å)		
C27—H27*A*	1.098	1.098
C27—H27*B*	1.098	1.097
C27—H27*C*	1.098	1.098
C28—H28*A*	1.101	1.101
C28—H28*B*	1.100	1.099
C28—H28*C*	1.097	1.097
C30—H30*A*	1.099	1.098
C30—H30*B*	1.099	1.099
C30—H30*C*	1.098	1.097
C31—H31*A*	1.101	1.100
C31—H31*B*	1.100	1.099
C31—H31*C*	1.100	1.099
N—H (riding model 0.88 Å)		
N1—H1	1.025	1.019

Table 4
Difference between X-ray (riding model) and DFT (calculated) bond lengths (%).

	CASTEP	*DMol*^{3}
Aryl C—H	14.1	14.1
Methyl C—H	11.9	11.8
Methine C—H	10.2	10.0
N—H	10.5	9.9

All H atoms were treated as riding, with C—H distances of 0.95 (aromatic), 0.98 (methyl) or 1.00 Å (aliphatic CH) and an N—H distance of 0.88 Å, and with $U_{iso}(H) = kU_{eq}$(carrier), where $k = 1.5$ for methyl groups and 1.2 otherwise. The isopropyl group (C26/C27/C28) was disordered over two sites. The anisotropic displacement parameters for corresponding partial-occupancy atoms were constrained to be the same. The corresponding bonded distances and 1,3 non-bonded distances in the two disorder components were restrained to be the same; the final site occupancies were 0.73 (3) and 0.27 (3).

CASTEP geometry optimization was performed using the generalized gradient corrected (GGA) exchange-correlation function of Perdew, Burke and Ernzerhof (PBE) (Perdew *et al.*, 1996). Ultrasoft pseudopotentials were used for all elements. The plane-wave basis set cutoff used was 310 eV. A single Γ point was used for Brillouin zone sampling; this setting is sufficiently accurate for such a large unit cell of an insulating material. The Broyden–Fletcher–Goldfarb–Shanno (BFGS) algorithm was used for the geometry optimization of the internal degrees of freedom. Calculations were considered converged when the maximum force on atoms was less than 0.01 eV Å^{-1}, the energy change was less than 5×10^{-6} eV per atom and the maximum atomic displacement was less than 5×10^{-4} Å.

DMol^3 geometry optimization also used the GGA PBE function with an all-electron core treatment and the double numerical plus polarization (DNP) basis set for atomic orbitals. Calculations were considered converged when the maximum force on atoms was less than 0.002 Ha Å^{-1}, the energy change was less than 1×10^{-5} Ha per atom and the maximum atomic displacement was less than 0.005 Å.

Data collection: *CrysAlis CCD* (Oxford Diffraction, 2006); cell refinement: *CrysAlis Pro* (Oxford Diffraction, 2010); data reduction: *CrysAlis Pro*; program(s) used to solve structure: *SIR92* (Altomare *et al.*, 1993); program(s) used to refine structure: *SHELXL97* (Sheldrick, 2008); molecular graphics: *ORTEP-3* (Farrugia, 1997); software used to prepare material for publication: *SHELXL97*, *PLATON* (Spek, 2009), *WinGX* (Farrugia, 1999) and *enCIFer* (Allen *et al.*, 2004).

The authors thank Dr David L. Hughes for access to the diffractometer. JAW and RHH thank the EPSRC for funding.

Supplementary data for this paper are available from the IUCr electronic archives (Reference: GD3345). Services for accessing these data are described at the back of the journal.

References

Accelrys (2009). *Materials Studio*. Version 5.0. Accelrys Inc., San Diego, California, USA.
Allen, F. H., Johnson, O., Shields, G. P., Smith, B. R. & Towler, M. (2004). *J. Appl. Cryst.* **37**, 335–338.
Altomare, A., Cascarano, G., Giacovazzo, C. & Guagliardi, A. (1993). *J. Appl. Cryst.* **26**, 343–350.
Clark, S. J., Segall, M. D., Pickard, C. J., Hasnip, P. J., Probert, M. J., Refson, K. & Payne, M. C. (2005). *Z. Kristallogr.* **220**, 567–570.
Cortright, S. B., Coalter, J. N. III, Pink, M. & Johnston, J. N. (2004). *Organometallics*, **23**, 5885–5888.
Cortright, S. B., Huffman, J. C., Yoder, R. A., Coalter, J. N. III & Johnston, J. N. (2004). *Organometallics*, **23**, 2238–2250.
Cortright, S. B. & Johnston, J. N. (2002). *Angew. Chem. Int. Ed.* **41**, 345–348.
Cortright, S. B., Yoder, R. A. & Johnston, J. N. (2004). *Heterocycles*, **62**, 223–227.
Delley, B. (2000). *J. Chem. Phys.* **113**, 7756–7764.
Farrugia, L. J. (1997). *J. Appl. Cryst.* **30**, 565.
Farrugia, L. J. (1999). *J. Appl. Cryst.* **32**, 837–838.
Milman, V. & Winkler, B. (2001). *Z. Kristallogr.* **216**, 99–104.
Oxford Diffraction (2006). *CrysAlis CCD*. Version 1.171. Oxford Diffraction Ltd, Abingdon, Oxfordshire, England.
Oxford Diffraction (2010). *CrysAlis Pro*. Version 1.171.33.55. Oxford Diffraction Ltd, Yarnton, Oxfordshire, England.
Perdew, J. P., Burke, K. & Ernzerhof, M. (1996). *Phys. Rev. Lett.* **77**, 3865–3868.
Sheldrick, G. M. (1997). *The SHELX97 Manual*. University of Göttingen, Germany.
Sheldrick, G. M. (2008). *Acta Cryst.* A**64**, 112–122.
Spek, A. L. (2009). *Acta Cryst.* D**65**, 148–155.